一般セッション(口頭講演) | 4 JSAP-Optica Joint Symposia 2023：4.7 Quantum Optics, Nonlinear Optics and Structured Optics

2023年9月22日(金) 9:00 ~ 10:45 | A310 (熊本城ホール)

[22a-A310-1~5] 4.7 Quantum Optics, Nonlinear Optics and Structured Optics

栗村 直(物材機構)

英語発表

9:00 ~ 9:30

[22a-A310-1] [JSAP-Optica Joint Symposia 2023 Invited Talk] Quantum information processing with continuous variables over optical fiber

〇Kuanshou Zhang[1,2], Jinxia Feng[1,2], Yuanji Li[1,2] (1.State Key Lab. of Quantum Optics and Quantum Optics Devices, Inst. of Opto-Electronics, Shanxi Univ., 2.Collaborative Innovation Center of Extreme Optics, Shanxi Univ.)

英語発表

9:30 ~ 10:00

[22a-A310-2] [JSAP-Optica Joint Symposia 2023 Invited Talk] Versatile quantum state tomography of photonic states via Hong-Ou-Mandel Interference

〇Yoshiaki Tsujimoto[1], Rikizo Ikuta[2], Kentaro Wakui[1], Toshiki Kobayashi[2], Mikio Fujiwara[1] (1.NICT, 2.Osaka univ.)

英語発表

10:00 ~ 10:15

[22a-A310-3] Observation of linewidth of electromagnetically induced transparency with temperature

〇(D)Anju Pal[1], Ajay Wasan[1] (1.IIT Roorkee)

奨励賞エントリー 英語発表

10:15 ~ 10:30

[22a-A310-4] Quantum-enhanced stimulated Raman scattering imaging in dual-polarization scheme

〇Zicong Xu[1], Kenichi Oguchi[1], Sho Nitanai[1], Yoshitaka Taguchi[1], Yuki Sano[1], Yasuyuki Ozeki[1] (1.Univ. of Tokyo)

英語発表

10:30 ~ 10:45

[22a-A310-5] Demonstration of Broad and Flat Optical Frequency Comb Generator by Employing Highly Non Linear Optical Fiber

〇(DC)PRIYANKA VERMA[1], SUKHBIR SINGH[1] (1.NETAJI SUBHAS UNIVERSITY OF TECHNOLOGY, DWARKA, SECTOR-3, DELHI-110078)

Quantum information processing with continuous variables over optical fiber

Kuanshou Zhang [1,2], Jinxia Feng [1,2], Yuanji Li [1,2]

[1] State Key Laboratory of Quantum Optics and Quantum Optics Devices, institute of Opto-Electronics, Shanxi University, Taiyuan, Shanxi, 030006, People's Republic of China

[2] Collaborative Innovation Center of Extreme Optics, Shanxi University, Taiyuan, Shanxi, 030006, People's Republic of China

E-mail: kuanshou@sxu.edu.cn

Metropolitan fiber quantum communication network is the key step to construct quantum communication network. Owing to continuous variable (CV) quantum entangled states of optical field can be generated unconditionally and deterministically, high-performance quantum information processing with continuous variables based on quantum states of optical field can be achieved. However, quantum information processing with continuous variable over optical fiber is a great challenge.

The entanglement robustness of EPR entangled state distributed over the single-channel and dual-channel optical fiber channel was investigated. It is found that in order to maintain the entanglement robustness of the EPR entangled state in lossy optical fiber channels, the dual-channel scheme has more stringent requirements on the correlation quadrature symmetry and purity of the initial entangled state than the single-channel scheme. In the single-channel scheme, the maximum transmission distance and robustness of the EPR entangled states with asymmetric modes is not sensitive to the asymmetry between modes. The change of asymmetry between modes does not lead to disentanglement. The maximum transmission distance does also not change. Distribution of CV entanglement at a telecommunication wavelength of 1550 nm over single mode fibers are realized experimentally. Entangled beams with quantum entanglement of 8.3 dB is generated using a single nondegenerate optical parametric amplifier based on a type-II periodically poled $KTiOPO_4$ crystal. When one beam of the generated EPR-entangled beams is distributed over 20 km of single mode fiber, 1.02 dB quantum entanglement can still be measured.

A real time deterministic quantum teleportation over a single fiber channel were presented. The effects of the transmission distance, the extra noise in the optical fiber, and the transmission efficiency of the lossy channel on the fidelity of deterministic quantum teleportation over a single optical fiber channel are theoretically analyzed. The real time deterministic quantum teleportation over a single fiber channel by exploiting the generated 1.5 μm EPR entanglement is experimentally implemented. The maximum transmission distance of the deterministic quantum teleportation is 10 km with the fidelity of 0.51 ± 0.01, which is higher than the classical teleportation limit of 1/2.

Versatile quantum state tomography of photonic states via Hong-Ou-Mandel interference

NICT [1], Osaka univ. [2], °Yoshiaki Tsujimoto[1], Rikizo Ikuta[2], Kentaro Wakui[1], Toshiki Kobayashi[2] and Mikio Fujiwara[1]

E-mail: tsujimoto@nict.go.jp

Hong-Ou-Mandel (HOM) interference [1] is a bunching phenomenon based on the bosonic nature of photons. When two photons that are perfectly indistinguishable from each other are mixed using a half beam splitter (HBS), they always bunch and exhibit the absence of coincidence resulting in a specific interferogram called HOM dip. The important property of the HOM interference is that the decrease in coincidence reflects the degree of indistinguishability of the input photons, i.e., it provides information regarding the probability of overlap of the input photons. Thus, this property should enable the estimation of a target photon in an unknown quantum state using a probe photon in a known state. In this work, we realize the above concept as the quantum state tomography (QST) applicable to d-dimensional photonic qudits, which we call HOM-QST [2]. Interestingly, we observe that HOM-QST is robust against various imperfections and that the probe photon can be replaced by classical light. Furthermore, we confirm this by demonstrating a proof-of-principle experiment using two-dimensional polarization qubits.

The concept of the HOM-QST is shown in Fig.1(a). For simplicity, we consider the HOM-QST of a polarization qubit as an example. The target photon under test and the probe photon in known polarization state are mixed by a HBS followed by a coincidence measurement. By denoting the polarization of the target photon and probe photon by ρ and k, respectively, the depth of the HOM dip is given by

$$\Delta_k = \frac{\eta n_s n_p}{2}\rho_k$$

where η is a product of the quantum efficiencies of the detectors, n_s and n_p are the average photon numbers of the target photon and probe photon, respectively. $\rho_k = \langle k|\rho|k\rangle$ is the probability of the k-polarized portion of the target photon. Here, $|k\rangle$ is the k-polarized single-photon state. The feature of HOM-QST is that no prior knowledge of the probe light is needed, such as n_p and its intensity correlation function $g^{(2)}(0)$; moreover, there is no theoretical requirement on these values. We perform the proof-of-principle demonstration of the HOM-QST of polarization qubits. We prepare diagonally (D) polarized heralded single photons as the target and compare the estimation results obtained by the conventional QST [3] with HOM-QST using a laser-light probe. The real parts of the reconstructed density matrices are shown in Fig.1 (b) and (c). The estimated fidelity (F) by HOM-QST is above F=0.99. Hence, it is shown that, regardless of the values of n_p and $g^{(2)}(0)$, HOM-QST can realize the precise estimation as our theoretical prediction. Our method serves as an alternative to perform the QST with a passive measurement setup and is applicable to QST of various degrees of freedom.

References

[1] C. K. Hong, Z.Y. Ou and L. Mandel, Phys. Rev. Lett. **59**, 2044 (1987).

[2] Y. Tsujimoto, R. Ikuta, K. Wakui, T. Kobayashi and M. Fujiwara, Phys. Rev. Applied **19**, 014008 (2023).

[3] D. F. V. James, *et al.*, Phys. Rev. A **64**, 052312 (2001).

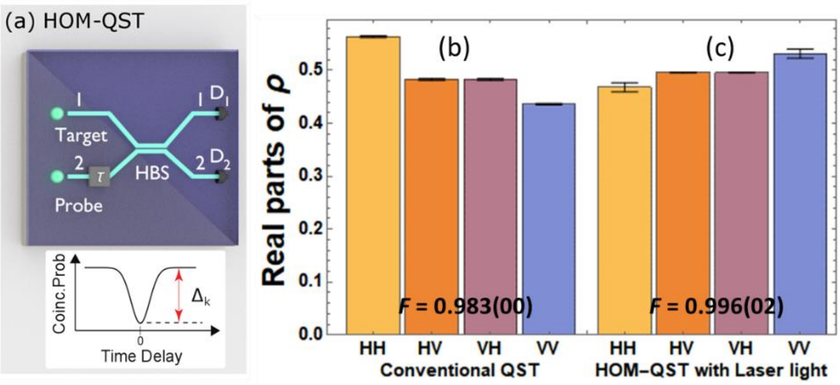

Fig.1 (a) The model of the HOM-QST. (b, c) Estimated density matrices of D-polarized target state using conventional QST (b) and HOM-QST with laser-light probe (c). The label "HV" indicates $\mathrm{Re}\langle H|\rho|V\rangle$ for example.

Observation of linewidth of electromagnetically induced transparency with temperature

Anju Pal[1],* and Ajay Wasan[1]
[1]Department of Physics, Indian Institute of Technology, Roorkee, 247667, India
*apal@ph.iitr.ac.in

I. INTRODUCTION

The EIT linewidth plays an important role in high-precision spectroscopy. The EIT linewidth depends on the parameters like laser intensity, doppler broadening and atomic relaxation, etc. In this study, we have observed the dependence of EIT linewidth on the temperature in the D2 transition of ^{87}Rb. The optical density increases with the increase of temperature, which has application in light storage [1], [2].

II. EXPERIMENTAL SETUP

The schematic of the experimental setup and the relevant energy level diagram is shown in Fig. 1 (a and b). In the present experiment, we used two external cavity diode lasers (ECDL) operated independently at wavelength 780 nm as probe and pump lasers. The pump laser was locked at the transition $F_g = 2 \leftrightarrow \mathrm{F}_e = 2$ while the probe laser was scanned around the transition $F_g = 1 \leftrightarrow \mathrm{F}_e = 2$ as shown in fig.1 (b).

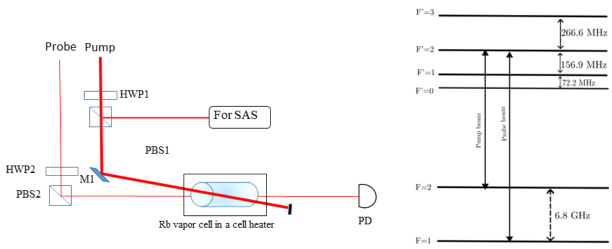

Fig. 1: Schematic diagram of the experimental setup and the corresponding energy level diagram.

Both lasers were passed through the Rb vapor cell in a co-propagating direction. The Rb vapor cell contains both the isotopes of Rb atoms (72% of ^{85}Rb and 28% of ^{87}Rb) and is placed inside a cell heater (THORLABS, GCH25-75). The temperature of the cell heater was controlled using the temperature controller (THORLABS, TC200). After the vapor cell, the probe laser was then monitored by a photodiode and oscilloscope. The probe and pump laser powers was fixed at 0.7 mW and 3.5 mW, respectively.

III. RESULTS AND DISCUSSION

Fig.2 shows the experimentally obtained results in a Λ-type system using D2 transition of ^{87}Rb atoms. To observe the effect of temperature on the EIT, we vary the cell temperature from 22C to 60C. We observed the VSOP dips due to the optical pumping of the pump beam.

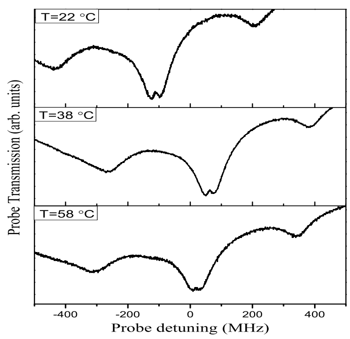

Fig. 2: Experimental results showing probe transmission at different temperatures.

The EIT peak emerged at the central VSOP dip. At a higher temperature, the optical density increases within the cell. So with the increase of optical density, the spontaneously emitted photon increases, which is reabsorbed by the dark state. So the decay rates associated with the ground state increase. Also, atom-atom collision and collision of atoms with the glass cell increases the ground state decay rates. This leads to a reduction in amplitude and an increase in the linewidth of the EIT Window.

IV. CONCLUSION

In conclusion, we have observed the increased amplitude and reduction in linewidth of EIT window with increased cell temperature.

References

[1] Das, Chandan et al., Physica Scripta, 97, 095401, 9 (2022)
[2] Phillips, David F et al., Physical Review Letters, 5, 783 (2008)

Quantum-enhanced stimulated Raman scattering imaging in dual-polarization scheme

Zicong Xu, Kenichi Oguchi, Sho Nitanai, Yoshitaka Taguchi, Yuki Sano, Yasuyuki Ozeki

Research Center for Advanced Science and Technology, The University of Tokyo,
4-6-1 Komaba, Meguro-ku, Tokyo 153-8904, Japan
E-mail: xuzicong19@g.ecc.u-tokyo.ac.jp

1. Introduction

Benefitting from the sub-Poissonian statistics, squeezed light has been applied to push the shot-noise-limited sensitivity of stimulated Raman scattering spectroscopy and microscopy to a sub-shot-noise level [1-4]. To surpass the sensitivity of state-of-the-art SRS microscopes, producing high-power squeezed light is desired. Quantum-enhanced balanced detection offers advantages for high-power operation by combining squeezed vacuum with a high-power local oscillator on a symmetric beamsplitter [5]. However, the balanced detection regime requires a high squeezing level to counteract the 3-dB signal-to-noise ratio (SNR) drawback. In this presentation, we introduce dual-polarization quantum-enhanced stimulated Raman scattering (QESRS), which is also suitable for high-power operation [6]. This approach utilizes a symmetric beamsplitter but detects squeezed light on two independent photodetectors, thus avoiding the 3-dB decrease in SNR.

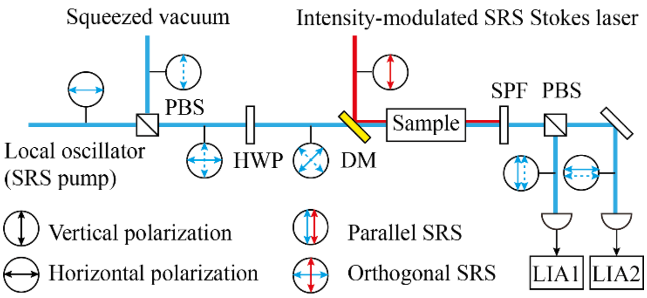

Fig. 1. Schematic of the experimental setup. PBS: polarizing beamsplitter, HWP: half-wave plate, DM: dichroic mirror, SPF: shortpass filter, LIA: lock-in amplifier.

2. Method and experimental setup

Fig. 1 shows the schematic of dual-polarization QESRS. Initially, squeezed vacuum and local oscillator are combined on a polarizing beamsplitter (PBS). The polarizing angles of both are rotated by 45 degrees using a half-wave plate before being directed towards the sample. By introducing an intensity-modulated vertically polarized Stokes laser, parallel and orthogonal SRS can occur simultaneously, resulting in an intensity modulation transferred to the pump laser [7]. At the detection stage, the QESRS signals from the two polarization channels are separated by another PBS and subsequently demodulated by two lock-in amplifiers.

3. Results

Figs. 2(a,b) provide a comparison between classical SRS and QESRS images obtained by blocking or unblocking the squeezed vacuum. The QESRS image demonstrates higher image contrast than the classical one. Figs. 2(c,d) illustrate the noise reduction level of QESRS images at different wavenumbers by sweeping the wavelength of the Stokes laser. Both parallel and orthogonal SRS measurements exhibit an average improvement of 0.5 dB in SNR.

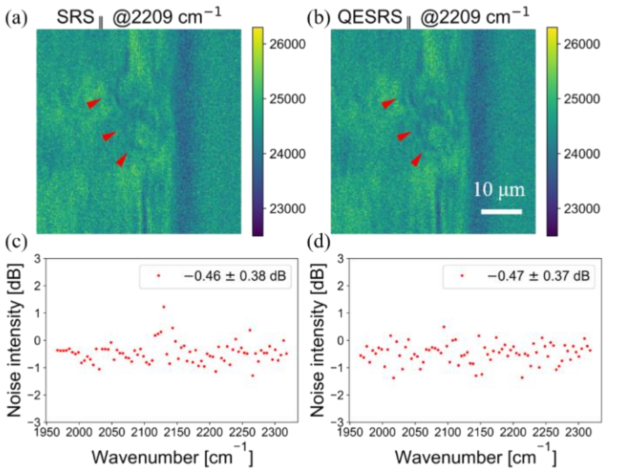

Fig. 2. (a,b) Examples of classical SRS and QESRS images at 2209 cm^{-1} in parallel SRS measurement. (c,d) Plots of noise reduction level at each wavenumber for (c) parallel and (d) orthogonal SRS measurements.

4. Conclusion

In this report, we have presented dual-polarization QESRS that can be operated in a high-power regime (14 mW). We demonstrate the feasibility of achieving sub-shot-noise sensitivity in two polarization channels while achieving a moderate level of noise reduction. This method shows promise for applications in other quantum-enhanced and polarization-resolved measurements as well.

References

[1] R. B. de Andrade, *et al.*, Optica **7**(5), 470 (2020).
[2] C. A. Casacio, *et al.*, Nature **594**(7862), 201 (2021).
[3] Z. Xu, *et al.*, Opt. Express **30**(11), 18589 (2022).
[4] Z. Xu, *et al.*, Opt. Lett. **47**(22), 5829 (2022).
[5] Y. Ozeki, *et al.*, J. Opt. Soc. Am. B **37**(11), 3288 (2020).
[6] Z. Xu, *et al.*, Appl. Phys. Lett., submitted (2023).
[7] J. Shou, *et al.*, Appl. Phys. Lett. **113**(3), 033701 (2018).

Demonstration of Broad and Flat Optical Frequency Comb Generator by Employing Highly Non Linear Optical Fiber

Priyanka Verma[1], Sukhbir Singh[1]
[1]Department of Electronics and Communication Engineering, Netaji Subhas University of Technology, Delhi, India
E-mail: priyanka.verma.phd21@nsut.ac.in

1. Introduction

The optical frequency comb (OFC) is prospective technique that can hike up the communication carrying capability of wide range in optical fiber communication [1]. Due to its numerous applications, including ultra-short pulse generation for different wavelength [2] multi-wavelength ultra-fast photonic signal processing, high-accuracy optoelectronic detectors and wavelength division multiplexing [3, 4], it draws attention of researchers. A collection of spectral lines is produced by a continuous laser source modulating a radio frequency signal. This manuscript proposed an effective technique for generation of OFC with cascading of modulators with Highly Nonlinear Fiber (HNLF) that produces coherent and highly spectral comb lines.

2. Proposed system setup for OFC

The CW laser pump depicts in Fig.1 at 1553nm produce unmodulated signal which passes through Electro Absorption Modulator (EAM) to enhance the intensity of laser light with 10GHz RF Source. The shape of spectrum get further enhanced by cascading of two Mach Zehnder Modulator (MZM) at -1V and 4V biasing voltage. The modulator 1 is intensity modulator, however modulator 2 work as phase modulator. The electrical inputs of MZM such as V_{DC} and V_{RF} drive two phase shifters to modulate E_{in} into two arms of modulator which are recombined to give E_{out} where γ is power splitting ratio. This is governed by equation given by (1) [5].

$$Eout(t) = \frac{Ein}{2}\left[\gamma e^{j\pi\left(\frac{V_{RF}(t)}{V_{\pi RF}}+\frac{V_{dc}}{V_{\pi dc1}}\right)} + (1-\gamma)e^{j\pi\frac{-V_{RF}(t)}{V_{\pi RF}}}\right] \quad (1)$$

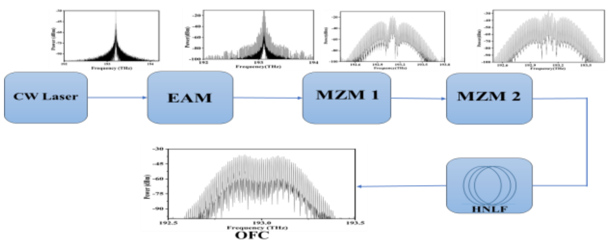

Fig. 1 OFC Generation by employing HNLF

The pulse train gets enhanced with nonlinear index of refraction of HNLF which gives additional optical spectral lines over a high bandwidth range which is governed in equation (2), where γ represents fiber nonlinear coefficient, n_2 is nonlinear index of refraction whereas A_{eff} is effective area of optical fiber and λ is operating wavelength.

$$\gamma = \frac{2\pi n_2}{\lambda A_{eff}} \quad (2)$$

3. Result and Discussion

The performance of generated optical frequency comb is analyzed with Optical Spectrum Analyzer (OSA) in optisystem. The stability is improved with cascading of modulator with RF source of 30GHz. The output spectrum at cascading of modulators is illustrated in Fig. 2 (a) & (b) respectively.

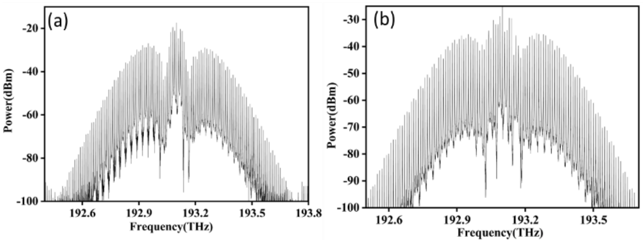

Fig. 2 Modulated Spectrum at (a) MZM 1(b) MZM 2.

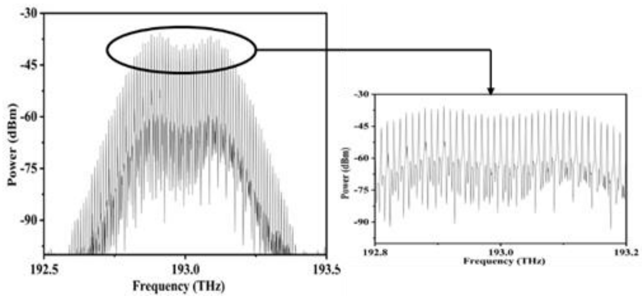

Fig. 3 Optical Frequency Comb Generation at Output of HNLF

The Fig.3 depicts generated OFC at output of HNLF. The obtained comb lines are 45 which is shown in circular image with 3dB flatness.

4. Conclusion

The proposed technique is effective with 45 numbers of comb lines and 3dB maximum power deviation. HNLF plays a vital role by enabling the nonlinear process that broadens and spread the spectral energy resulting in a comb like structure with evenly spaced frequency lines. The comb generated is valuable for a variety of applications such as frequency metrology and communication network.

References

[1] A. Parriaux, K. Hammani, and G. Millot, "Electro-optic frequency combs," *Advances in Optics and Photonics*, vol. 12, pp. 223-287, 2020.

[2] T. Yang, J. Dong, S. Liao, D. Huang, and X. Zhang, "Comparison analysis of optical frequency comb generation with nonlinear effects in highly nonlinear fibers," *Optics express*, vol. 21, pp. 8508-8520, 2013.

[3] R. Ullah, B. Liu, Q. Zhang, Q. Tian, F. Tian, Z. Qu, *et al.*, "Optical frequency comb generation with high tone-to-noise ratio for large-capacity wavelength division multiplexed passive optical network," *Optical Engineering*, vol. 54, pp. 116102-116102, 2015.

[4] C. Lei, H. Chen, M. Chen, S. Yang, and S. Xie, "Recirculating frequency shifting based wideband optical frequency comb generation by phase coherence control," *IEEE Photonics Journal*, vol. 7, pp. 1-7, 2014.

[5] J. Cartledge, C. Rolland, S. Lemerle, and A. Solheim, "Theoretical performance of 10 Gb/s lightwave systems using a III-V semiconductor Mach-Zehnder modulator," *IEEE photonics technology letters*, vol. 6, pp. 282-284, 1994.